COMMUNICATIONS IN NUMERICAL METHODS IN ENGINEERING
Commun. Numer. Meth. Engng, **15**, 283–293 (1999)

CONSISTENT DISCRETIZATION OF THICKNESS STRAINS IN THIN SHELLS INCLUDING 3D-MATERIAL MODELS

C. HUETTEL AND A. MATZENMILLER*
Universitaet GH Kassel, Institute for Mechanics, Moenchebergstr. 7, D-34109 Kassel, Germany

SUMMARY

Following an idea by Büchter *et al.* (1994), the normal strain in the thickness direction of shells with inextensible directors is accounted for by the EAS-method, in order to enforce for arbitrary 3D-material models the zero normal stress-condition in the average sense. In the present paper a polynomial expansion of the normal strain interpolation in the thickness direction including the constant term is proposed. This extension is consistent with Simo and Rifai (1990). The proposed method is also suitable to analyse plane stress problems with arbitrary 3D-material models. Copyright © 1999 John Wiley & Sons, Ltd.

KEY WORDS EAS-method; thickness strains; inextensible shell director; consistent strain interpolation

1. INTRODUCTION

The enhanced assumed strain (EAS-) method, as outlined in Reference 1, is applied in Reference 2 to account for the normal strain in thickness direction of shell models with the assumption of an inextensible director. The well-known displacement approach is extended by means of the EAS-method in order to enforce the zero normal stress condition in the weak sense for shell formulations with arbitrary 3D-material models. However, the discretized field of incompatible strains in the thickness direction becomes zero according to the proposal in Reference 2 even in the case of spatially constant strains for elements with a constant Jacobian determinant. Spatially constant strain fields in the shell body are caused by homogeneous membrane deformations of plane shells. In the present approach the thickness strains are only represented by the incompatible part, which include constant strain fields. Hence, the related strain discretization must include a constant term in the polynomial expansion. Otherwise, the membrane part of the deformation is represented erroneously such as would be the case if the procedure in Reference 2 were applied to the shell formulation here. In the present paper the polynomial expansion of the normal strain interpolation in the thickness direction with a constant strain term is studied, giving correct results also for the membrane strains in states of homogeneous deformations, independently on the shape of the elements.

* Correspondence to: A. Matzenmiller, Institut fur Mechanik, Universitat Gesamthoschschule Kassel, Moenchebergstr. 7, D-34109 Kassel, Germany.

CCC 1069–8299/99/040283–11$17·50

Received 23 March 1998
Accepted 4 August 1998

2. KINEMATICS OF PLATES AND SHELLS

The position vector $\boldsymbol{p}$ of an arbitrary point within the shell-continuum is described by the position vector of the reference surface $\boldsymbol{x}$ and a relative distance in thickness direction, described by the unit vector $\boldsymbol{d}$, also denoted as the normalized shell director:

$$\boldsymbol{p}(\theta^1, \theta^2, \theta^3) = \boldsymbol{x}(\theta^1, \theta^2) + \kappa(\theta^1, \theta^2)\theta^3 \boldsymbol{d}(\theta^1, \theta^2) \in \mathcal{B} \quad \text{with} \quad |\boldsymbol{d}| = 1 \tag{1}$$

Herein, $(\theta^1, \theta^2, \theta^3)$ are curvilinear convective co-ordinates of the shell and $|\boldsymbol{d}| = \sqrt{(\boldsymbol{d} \cdot \boldsymbol{d})}$ is the Euclidean norm. κ is the relative thickness of the shell:

$$\kappa(\theta^1, \theta^2) = \frac{h(\theta^1, \theta^2)}{h_0}$$

where h is the actual and h_0 a constant reference thickness of the shell, both measured along the director. It holds for θ^3:

$$-\frac{h_0}{2} \leqslant \theta^3 \leqslant \frac{h_0}{2}$$

$\mathcal{B}$ is the volume occupied by the shell in the current state of deformation. The position vector of a point in the undeformed state $\mathcal{B}_0$ is marked with capital letters:

$$\boldsymbol{P}(\theta^1, \theta^2, \theta^3) = \boldsymbol{X}(\theta^1, \theta^2) + \mathcal{K}(\theta^1, \theta^2)\theta^3 \boldsymbol{D}(\theta^1, \theta^2) \in \mathcal{B}_0 \tag{2}$$

with $|\boldsymbol{D}| = 1$ and $\mathcal{K}(\theta^1, \theta^2) = H(\theta^1, \theta^2)/h_0$, where H is the initial thickness of the shell. The invariance assumption of the shell thickness under loading is approximately enforced by the condition

$$\kappa \equiv \mathcal{K} \;\leftrightarrow\; h \equiv H \tag{3}$$

i.e. the thickness, *measured along the director*, remains unchanged during deformation. Note, the kinematics of pure membrane deformation is comprised in (1) and (2) as the special case, where the director is always perpendicular to the midsurface of the shell during deformation.

The covariant base vectors of the shell are:

$$\begin{aligned} \boldsymbol{G}_\eta &= \frac{\partial \boldsymbol{P}}{\partial \theta^\eta} = \boldsymbol{X}_{,\eta} + \theta^3(\kappa \boldsymbol{D}_{,\eta} + \kappa_{,\eta}\boldsymbol{D}), \quad & \boldsymbol{G}_3 &= \frac{\partial \boldsymbol{P}}{\partial \theta^3} = \kappa \boldsymbol{D} \\ \boldsymbol{g}_\eta &= \frac{\partial \boldsymbol{p}}{\partial \theta^\eta} = \boldsymbol{x}_{,\eta} + \theta^3(\kappa \boldsymbol{d}_{,\eta} + \kappa_{,\eta}\boldsymbol{d}), \quad & \boldsymbol{g}_3 &= \frac{\partial \boldsymbol{p}}{\partial \theta^3} = \kappa \boldsymbol{d} \end{aligned} \tag{4}$$

where the short hand notation with the Greek index 'η' indicates partial differentiation with respect to either θ^1 or θ^2. The contravariant base vectors $\boldsymbol{G}^i$ are defined by

$$\boldsymbol{G}^i \cdot \boldsymbol{G}_j = \delta^i_j \text{ and } \delta^i_j = \begin{cases} 1 \text{ for } & i = j \\ 0 \text{ for } & i \neq j \end{cases}$$

where the Roman indices i and j take the integer values from 1 to 3. The second Piola–Kirchhoff stress tensor $\tilde{\boldsymbol{T}}$ and the Green strain tensor $\boldsymbol{E}$, refering to covariant or contravariant, bases as the case may be, read:

$$\begin{aligned}\tilde{\boldsymbol{T}} &= T^{ij}\boldsymbol{G}_i \otimes \boldsymbol{G}_j \\ \boldsymbol{E} &= E_{ij}\boldsymbol{G}^i \otimes \boldsymbol{G}^j = \tfrac{1}{2}(g_{ij} - G_{ij})\boldsymbol{G}^i \otimes \boldsymbol{G}^j\end{aligned} \tag{5}$$

where the summation convention applies for repeated indices. The covariant components of the metric tensors g_{ij} and G_{ij} are the scalar products of the covariant base vectors, e.g. $G_{ij} = \boldsymbol{G}_i \cdot \boldsymbol{G}_j$. Due to (4), (3) and $|\boldsymbol{D}| = |\boldsymbol{d}| = 1$ the strain component E_{33} vanishes identically:

$$E_{33} = \tfrac{1}{2}(g_{33} - G_{33}) = \tfrac{1}{2}(\kappa^2 \boldsymbol{d}\cdot\boldsymbol{d} - \mathcal{K}^2 \boldsymbol{D}\cdot\boldsymbol{D}) = 0 \tag{6}$$

Equation (3) and (6) represent a constraint for the stretch of the shell director in terms of E_{33} due to the displacement assumption of an inextensible director according to (1) and (2). Following an idea in Reference 2, the actual thickness strains $\tilde{E}_{33}$ are accounted for by the EAS-method according to Reference 1 in terms of an incompatible part $\tilde{\boldsymbol{E}}$ of the strain tensor as outlined in the following.

3. EXPANSION OF THE STRAINS

The compatible strains $\boldsymbol{E}$ according to (5) are complemented variationally consistent with an incompatible part by means of the EAS-method.[1] Since the incompatible strains do not need to be continuous across the interelement boundaries, the parameters of the incompatible part after discretization may be eliminated on the element level before the structural assemblage.

Let $\mathcal{B} \approx \cup_{e=1}^{n_{\text{elm}}} \mathcal{B}_e$ be a finite element discretization of the shell in terms of n_{elm} isoparametric shell elements. One-to-one mappings between element parameters (r, s, t) and curvilinear co-ordinates shall be given:

$$(r, s, t) \in [-1, 1]^3 \to (\theta_e^1(r, s), \theta_e^2(r, s), \theta_e^3(t)) \quad \text{with} \quad \theta_e^3(t) = \frac{h_0}{2} t$$

leading to

$$(r, s, t) \in [-1, 1]^3 \;\to\; \boldsymbol{p}_e = \boldsymbol{p}_e(r, s, t) \in \mathcal{B}_e$$

and

$$(r, s, t) \in [-1, 1]^3 \;\to\; \boldsymbol{P}_e = \boldsymbol{P}_e(r, s, t) \in \mathcal{B}_{e0}$$

The volume integrals in the sequel are obtained as in standard finite element procedures:

$$\int_V (\cdot)\mathrm{d}V = \sum_{e=1}^{n_{\text{elm}}} \int_{-1}^{1}\int_{-1}^{1}\int_{-1}^{1} (\cdot)_e J_e \,\mathrm{d}r\,\mathrm{d}s\,\mathrm{d}t \quad \text{with} \quad J_e = \left[\frac{\partial \boldsymbol{P}_e}{\partial r}, \frac{\partial \boldsymbol{P}_e}{\partial s}, \frac{\partial \boldsymbol{P}_e}{\partial t}\right] \tag{7}$$

where $[(\cdot), (\cdot), (\cdot)]$ represents the triple scalar product. The summation symbol and the index e will be omitted for convenience in the following.

The structure of the variational equations for the EAS-method is derived from the Hu–Washizu principle for the solution of boundary value problems with the three independent vector valued variables $\mathbf{y}$, $\boldsymbol{\alpha}$ and $\boldsymbol{\beta}$ for the parametrization of displacement-dependent strains $\boldsymbol{E}(\mathbf{y})$, incompatible strains $\tilde{\boldsymbol{E}}(\boldsymbol{\alpha})$ and stresses $\tilde{\boldsymbol{S}}(\boldsymbol{\beta})$:

$$\begin{aligned} \Pi(\mathbf{y}, \boldsymbol{\alpha}, \boldsymbol{\beta}) &= W_{\mathrm{i}}(\mathbf{y}, \boldsymbol{\alpha}, \boldsymbol{\beta}) - W_{\mathrm{a}}(\mathbf{y}) \rightarrow \text{stationary} \\ W_{\mathrm{i}}(\mathbf{y}, \boldsymbol{\alpha}, \boldsymbol{\beta}) &= \int_V \{w_{\mathrm{i}}[\boldsymbol{E}(\mathbf{y}) + \tilde{\boldsymbol{E}}(\boldsymbol{\alpha})] - \tilde{\boldsymbol{S}}(\boldsymbol{\beta}) \cdot \tilde{\boldsymbol{E}}(\boldsymbol{\alpha})\} \mathrm{d}V \end{aligned} \tag{8}$$

Π is the total energy of the shell, W_{i} is the internal work, W_{a} the external work of the applied forces and w_{i} the strain energy density function per unit initial volume. $\mathbf{y}$ is the vector of the nodal degrees of freedom of the shell displacements and rotations, $\boldsymbol{\alpha}$ a vector of nodeless parameters of the incompatible part of the strains $\tilde{\boldsymbol{E}}$ and $\boldsymbol{\beta}$ is a vector of nodeless parameters of the second Piola–Kirchhoff type stress tensor $\tilde{\boldsymbol{S}}$, which is independent of the constitutive assumption. The scalar product of two second-order tensors is defined by $\tilde{\boldsymbol{S}} \cdot \tilde{\boldsymbol{E}} = \mathrm{tr}(\tilde{\boldsymbol{S}}\tilde{\boldsymbol{E}}^{\mathrm{T}})$, where $\mathrm{tr}(\cdot)$ is the trace operator.

The stress field $\tilde{\boldsymbol{S}}$ shall be orthogonal to the incompatible strains, in the sense of the energy norm:

$$\int_V \tilde{\boldsymbol{S}}(\boldsymbol{\beta}) \cdot \tilde{\boldsymbol{E}}(\boldsymbol{\alpha}) \mathrm{d}\boldsymbol{V} = 0 \quad \forall \quad \boldsymbol{\alpha}, \boldsymbol{\beta} \tag{9}$$

Hence, the first variation of the functional (8) with respect to the independent variables reduces with the introduction of

$$\tilde{\boldsymbol{T}} := \frac{\partial w_{\mathrm{i}}(\bar{\boldsymbol{E}})}{\partial \bar{\boldsymbol{E}}} \quad \text{and} \quad \bar{\boldsymbol{E}} = \boldsymbol{E} + \tilde{\boldsymbol{E}} \tag{10}$$

to

$$\begin{aligned} \Pi_y &:= \delta\Pi(\mathbf{y}) = \int_V \tilde{\boldsymbol{T}} \cdot \delta\boldsymbol{E}(\mathbf{y}) \, \mathrm{d}V - \delta W_{\mathrm{a}}(\mathbf{y}) = 0 \quad \forall \quad \delta\mathbf{y} \\ \Pi_\alpha &:= \delta\Pi(\boldsymbol{\alpha}) = \int_V [\tilde{\boldsymbol{T}} \cdot \delta\tilde{\boldsymbol{E}}(\boldsymbol{\alpha})] \, \mathrm{d}V = 0 \quad \forall \quad \delta\boldsymbol{\alpha} \end{aligned} \tag{11}$$

The variations $\delta(\cdot)$ stand for the Gateaux derivatives

$$\delta(\cdot)(\mathbf{y}) = \mathrm{D}(\cdot)(\mathbf{y})[\delta\mathbf{y}] \text{ and } \delta(\cdot)(\boldsymbol{\alpha}) = \mathrm{D}(\cdot)(\boldsymbol{\alpha})[\delta\boldsymbol{\alpha}]$$

For example $\mathrm{D}\boldsymbol{E}(\mathbf{y})[\delta\mathbf{y}]$ is the derivative of $\boldsymbol{E}$ at $\boldsymbol{y}$ in the direction $\delta\mathbf{y}$. In order to ensure convergence and stability, the space $\mathcal{E}$ of standard compatible strains $\boldsymbol{E}$ must be disjoint from the space $\tilde{\mathcal{E}}$ of the incompatible strains Ẽ, i.e.

$$\mathcal{E} \cap \tilde{\mathcal{E}} = \emptyset \tag{12}$$

This condition is met trivially for any discretization of incompatible strains in thickness direction only

$$\tilde{\boldsymbol{E}}(\boldsymbol{\alpha}) = \tilde{E}_{33}(\boldsymbol{\alpha})\boldsymbol{G}^3 \otimes \boldsymbol{G}^3$$

due to (6).

In contrast to References 1 and 2 a complete linear polynomial expansion in element co-ordinates (r, s, t) with nodeless parameters $\boldsymbol{\alpha}$ is inserted into $\tilde{E}_{33}$ for the spatial discretization, also containing a constant term with parameter α_1 in this approach:

$$\tilde{E}_{33} = \boldsymbol{N}_{\alpha}\boldsymbol{\alpha} = \frac{J_0}{J}\{1, r, s, rs, t, rt, st, rst\}\{\alpha_1, \alpha_2, \alpha_3, \alpha_4, \alpha_5, \alpha_6, \alpha_7, \alpha_8\}^{\mathrm{T}} \tag{13}$$

where $J_0 := J(r = 0, s = 0, t = 0)$. Besides the discretization in (13), denoted as *complete expansion*, also the performance of the so-called *reduced expansion*

$$\tilde{E}_{33} = \frac{J_0}{J}\{1, t\}\{\alpha_1, \alpha_5\}^{\mathrm{T}} \tag{14}$$

is investigated in the numerical examples below. An expansion without the element $N_{\alpha 1}$:

$$\tilde{E}_{33} = \frac{J_0}{J}\{r, s, rs, t, rt, st, rst\}\{\alpha_2, \alpha_3, \alpha_4, \alpha_5, \alpha_6, \alpha_7, \alpha_8\}^{\mathrm{T}} \tag{15}$$

will be called an *incomplete expansion*. Using the incomplete expansion, the constant part in the normal through the thickness strains is missing due to (6) and (15). The incomplete expansion is only introduced in order to study the erroneous convergence of the approximate solutions with increasing mesh refinement in some examples. Therefore, the incomplete expansion is *not* recommended for applications.

The terms in (13) and (14), proportional to the thickness co-ordinate t, are needed for those states of shell-deformations where bending occurs. Then, the in-plane normal strains E_{11} or E_{22} vary through the thickness, necessitating at least a linear varying $\tilde{E}_{33}$ through the thickness due to Poisson's effect. Only in the absence of bending, i.e. in states of pure membrane deformations, do the terms proportional to the thickness co-ordinate t not contribute to the solution and may be omitted in (13) and (14).

The only non-trivial component of the incompatible stress field $\tilde{\boldsymbol{S}} = S^{33}\boldsymbol{G}_3 \otimes \boldsymbol{G}_3$ in (9) is S^{33}. The shape functions for the stresses S^{33} are constructed with polynomials such that the term $\tilde{\boldsymbol{S}} \cdot \tilde{\boldsymbol{E}}$ in (9) may be integrated exactly by the two-point Gauss-quadrature rule. Thus, the maximum order of the polynomial in the integrand $(\tilde{\boldsymbol{S}} \cdot \tilde{\boldsymbol{E}}J)$ of (9) and (7) must be $\leqslant 3$. The orthogonality condition in (9) with thickness strain $\tilde{E}_{33}$ according to (13) is satisfied, if at least one of the factors $1 - 3r^2$, $1 - 3s^2$ or $1 - 3t^2$ appears in each shape function for S^{33}. At all sampling points $(r, s, t) \in \{-1/\sqrt{3}, 1/\sqrt{3}\}^3$ of the integration rule for second-order Gauss-quadrature the stress $S^{33} = 0$ vanishes and it follows that

$$\int_V S^{33}\delta\bar{E}_{33}J \,\mathrm{d}r \,\mathrm{d}s \,\mathrm{d}t = 0$$

for the only non-zero stress component in the stress tensor $\tilde{\boldsymbol{S}}$. Hence, the variationally consistent stress recovery in Reference 1 with zero normal stresses at the sampling points satisfies the zero normal stress condition in the weak sense for the second-order Gauss-quadrature rule.

4. NUMERICAL EXAMPLES

The numerical examples are performed with the isoparametric 4-node shell element in Reference 3, implemented in the finite element program FEAP.[4] The shell director is described by the angles ψ and ε between the director and the x-axis, respectively the y-axis, according to the relations[3]

$$\mathbf{d} = \cos\psi\ \mathbf{e}_x + \sin\psi\cos\varepsilon\ \mathbf{e}_y + \sin\varepsilon\ \mathbf{e}_z$$

$$\cos\psi = \mathbf{d}\cdot\mathbf{e}_x \text{ and } \tan\varepsilon = \frac{\mathbf{d}\cdot\mathbf{e}_z}{\mathbf{d}\cdot\mathbf{e}_y}$$

The angles are interpolated with the standard isoparametric, bilinear shape functions N_y between the values ε^K and ψ^K at the four nodes according to

$$\varepsilon = \sum_{K=1}^{4} N_{\mathrm{y}}^K \varepsilon^K \quad \text{and} \quad \psi = \sum_{K=1}^{4} N_{\mathrm{y}}^K \psi^K$$

The vector $\mathbf{y}$ of the nodal degrees of freedom contains the nodal co-ordinates of the reference surface of the shell and the angles ε and ψ:

$$\mathbf{y}^K = (\mathrm{x}_1^K, \mathrm{x}_2^K, \mathrm{x}_3^K, \varepsilon^K, \psi^K) \quad \text{with} \quad x^K = \mathrm{x}_1^K \mathbf{e}_x + \mathrm{x}_2^K \mathbf{e}_y + \mathrm{x}_3^K \mathbf{e}_z$$

The transverse shear strain interpolation in the shell element follows the 'assumed strain' concept in References 5 and 6. The integrals in (11) are evaluated numerically with two point Gauss-quadrature in each dimension.

Besides the isotropic linear elastic Hooke/St. Venant material, for which a degenerated version with $T^{33} = 0$ exists, an isotropic, non-linear, hyperelastic model

$$\tilde{\boldsymbol{T}} = \mu\mathbf{1} + \left(\frac{\lambda}{2}\ln\det\boldsymbol{C} - \mu\right)\boldsymbol{C}^{-1}, \text{ with } \quad \mu = \frac{E}{2(1+\nu)} \quad \text{and} \quad \lambda = \frac{2\nu\mu}{1-2\nu} \tag{16}$$

according to Simo–Pister[7] is used. $\boldsymbol{C}$ is the right Cauchy–Green tensor, obtained from $\boldsymbol{C} = 2\bar{\boldsymbol{E}} + \mathbf{1}$ in the case of the EAS-formulation. E is Young's modulus and ν Poisson's ratio. The material model in (16) turns into the Hooke/St. Venant relation in the case of infinitely small deformations.

In addition, the generalized plasticity model of Reference 8 in the version of Reference 9 is implemented into the shell element for small strain applications. The constitutive equations may be summarized as follows:

$$\boldsymbol{E} = \boldsymbol{E}_{\mathrm{e}} + \boldsymbol{E}_{\mathrm{p}} \tag{17}$$

$$\dot{\boldsymbol{E}}_{\mathrm{p}} = \begin{cases} \dot{\gamma}\boldsymbol{N}: & \text{plastic loading} \\ \mathbf{0}: & \text{else} \end{cases} \tag{18}$$

$$\boldsymbol{T} = K\ \mathrm{tr}(\boldsymbol{E}_{\mathrm{e}})\mathbf{1} + 2\mu\boldsymbol{E}_{\mathrm{e}}^{\mathrm{D}} \tag{19}$$

$$\dot{s} = \sqrt{\tfrac{2}{3}}\|\dot{\mathbf{E}}_{\mathrm{p}}\| \tag{20}$$

$$\dot{\boldsymbol{X}} = c\dot{\boldsymbol{E}}_{\mathrm{p}} - b\boldsymbol{X}\dot{s} \tag{21}$$

$$f = \|(\boldsymbol{T} - \boldsymbol{X})^{\mathrm{D}}\| \text{-} \sqrt{\tfrac{2}{3}}k(s) \lesseqgtr 0 \tag{22}$$

$$k(s) = k_{\infty} + (k_0 - k_{\infty})\mathrm{e}^{-\alpha s} \tag{23}$$

$$\boldsymbol{N} = \frac{\partial f}{\partial \boldsymbol{T}} = \frac{(\boldsymbol{T} - \boldsymbol{X})^{\mathrm{D}}}{\|(\boldsymbol{T} - \boldsymbol{X})^{\mathrm{D}}\|} \tag{24}$$

$$F = h(f)\dot{f} - g(s)\dot{s} = 0 \tag{25}$$

$$\boldsymbol{N}\cdot\dot{\boldsymbol{T}} \geqslant 0 \quad \text{and} \quad f \geqslant 0 \rightarrow \text{plastic loading}$$

$$\boldsymbol{N}\cdot\dot{\boldsymbol{T}} < 0 \quad \text{or} \quad f < 0 \rightarrow \text{elastic behaviour}$$

Equations (17)–(24) define classical J_2-plasticity with linear, isotropic elasticity. Equation (19) represents the linear elastic stress–strain relations with K and μ as the elasticity moduli and $(\ )^{\mathrm{D}}$ as the deviator. Equations (18) and (24) establish the evolution of the plastic strains according to the normality rule with $\dot{\gamma}$ as the plastic multiplier. The norm of a second-order tensor is defined by the scalar product: $\|(\cdot)\| = \sqrt{(\cdot)\cdot(\cdot)}$. Equation (21) gives the non-linear Armstrong–Frederick type evolution of the back stresses $\boldsymbol{X}$ with parameters b and c. Equations (20) and (23) define the plastic arclength s and non-linear, isotropic hardening variable $k(s)$ with material parameters k_0, k_{∞} and α. Since the yield function f in (22) may take positive values during plastic loading, which is a special feature of the generalized plasticity model, an evolutionary equation for the yield function is needed in the case of plastic loading. This equation is supplied by (25) by means of functions $h(f)$ and $g(s)$, given as

$$h(f) = \frac{\delta f}{f_{\infty} - f} \quad \text{and} \quad g(s) = 1$$

with material parameters δ and f_{∞}. A degenerated version with $T_{33} = 0$ exists for this material for small strain plasticity.[9] The material parameters E, ν, b, c and k_0 for the XCrNi18·9 steel, as indicated in Reference 10, p. 97, are summarized in Table I. δ and f_{∞} are reasonably chosen parameters for generalized plasticity.

4.1 Cantilever Beam

The cantilever beam of Figure 1 consists of a linear elastic Hooke/St. Venant material with $E = 200{,}000$ MPa and $\nu = 0{\cdot}3$. The beam is loaded at its free end by the force $F_x = 200$ N in the longitudinal direction and a bending moment of $M_y = 32$ Nmm. The displacements of the free end, obtained from the geometrically linear calculation, are presented in Table II for different models.

The incomplete expansion for the discretization of thickness strains as in (15) yields an incorrect displacement u_x in the x-direction, given in column D, as well as it does in the non-generated model — see the results in columns D and E. All expansions, containing the constant term α_1 as in (13) and (14) result in the correct displacements at the free end of the beam — see columns A, B and C. Due to the uniform mesh with rectangular elements chosen and the

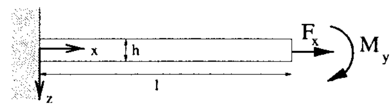

Figure 1. Cantilever beam

Table I. Material parameters for the generalized plasticity model

Parameter	E	ν	b	c	k_0	δ	f_∞
Unit	MPa	–	–	MPa	MPa	–	MPa
Value	208000	0·3	525·5	41078	170	0·01	20

Table II. Results of the geometrically linear calculation

	Hooke/St. Venant material				
	Degenerated	Not degenerated			
		With EAS-expansion in			Without EAS
	A	(13) B	(14) C	(15) D	E
u_x[mm]	0·01	0·01	0·01	0·0091	0·0091
u_z[mm]	0·96	0·96	0·96	0·96	0·8736

constant stress and strain state in the direction of the beam axis, the expansions with the parameters α_2 to α_4 and α_6 and α_8 do not influence the results — see columns B and C.

4.2. *Shearing of a rectangular panel*

The panel in Figure 2 is subjected to a displacement driven shear test. The original thickness of the panel is 1 mm. The material parameters of the Simo–Pister model are $E = 1000$ MPa and $\nu = 0{\cdot}45$. The displacements of the two upper edges are $u_x = 48$ mm in the horizontal and $u_y = -24$ mm in the vertical direction. An 'exact' solution for this boundary value problem is given in the Appendix. The stress and strain components at the sampling points of the Gauss-quadrature rule are referred to the Cartesian frame for the finite strain calculation with the complete linear EAS-expansion in (13). The values of the Green-strains (ε_{ij}) and second Piola–Kirchhoff-stresses (σ_{ij}) from (16) differ at most by less than 10^{-10} from the values displayed in Table III. The 'exact' result in plane stress is also given in Table III.

It is noted from the analysis that:

- the numerical solution obtained from the complete EAS-expansion is in excellent agreement with the 'exact' results
- the normal stress in the thickness direction vanishes up to machine precision
- the strains as well as the stresses are constant throughout the deformed panel

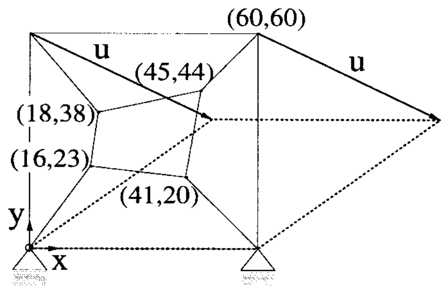

Figure 2. Shearing test

4.3. Cook's Membrane

In-plane shearing of a tapered panel, clamped at one edge, is considered. The boundary value problem with its dimensions in mm is sketched in Figure 3. The displacements are magnified by a factor of ten. The panel has a thickness of 1 mm and the uniform line load at the free edge **q** is 80 N/mm. Generalized plasticity is used for the material model with parameters as given in Table I. The vertical displacement of the upper right corner of the panel is plotted vs. the number of elements per side in Figure 4. Obviously, the non-degenerated model with the complete EAS-expansion gives the same displacements as the degenerated model does, independently of the number of elements per side.

The superiority of the complete expansion of thickness strain interpolation with respect to the reduced expansion diminishes with increasing refinement of the mesh, due to the decreasing differences of the stresses and strains within the elements.

5. SUMMARY

The EAS-method, as presented in Reference 1, is consistently applied to the kinematic assumption of shells with an inextensible director. A constant term is introduced into the discretization

Table III. Stresses and strains

Component	FEAP	'Exact'
ε_{xx} [%]	0	0
ε_{yy} [%]	0	0
ε_{zz} [%]	57·5457	57·5457
ε_{xy} [%]	40	40
ε_{xz} [%]	0	0
ε_{zx} [%]	0	0
σ_{xx} [MPa]	−1715·43	−1715·43
σ_{yy} [MPa]	−1715·43	−1715·43
σ_{zz} [MPa]	0	0
σ_{xy} [MPa]	1648·21	1648·21
σ_{xz} [MPa]	0	0
σ_{yz} [MPa]	0	0

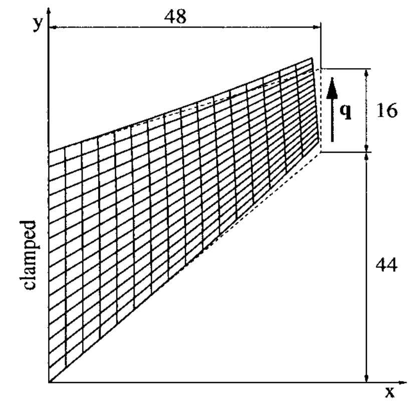

Figure 3. Cook's Membrane

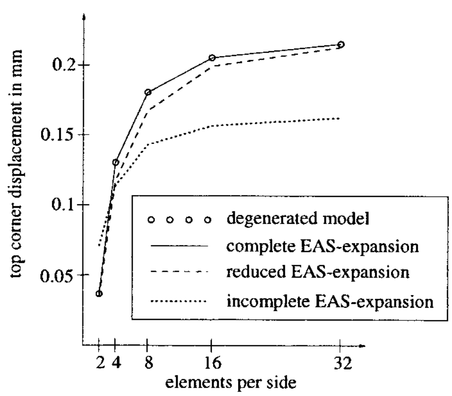

Figure 4. Displacement

for the incompatible normal strain field in the thickness direction in order to enforce the zero normal stress condition in the weak sense.

The proposed expansion allows for the incorporation of arbitrary three-dimensional material models into shell formulations. The capability of the shell element to satisfy the patch test and the zero normal stress constraint in the weak sense is shown in the numerical examples. For nearly rectangular elements or fine element meshes an EAS-expansion with only two parameters is sufficient.

APPENDIX: SHEAR TEST

The solution for the boundary value problem in Figure 2 is derived. The displacement field is given as

$$\boldsymbol{p} = [X + Y \sin \alpha]\boldsymbol{e}_x + Y \cos(\alpha)\boldsymbol{e}_y + \beta Z \boldsymbol{e}_z \quad \text{with} \quad \boldsymbol{P} = \mathrm{X}\boldsymbol{e}_x + \mathrm{Y}\boldsymbol{e}_y + Z\boldsymbol{e}_z$$

For the chosen values of $\sin \alpha = 0{\cdot}8$ and $\cos \alpha = 0{\cdot}6$ only the quantity β is unknown. From the assumed displacement field the deformation gradient $\boldsymbol{F}$, the right-Cauchy–Green tensor $\boldsymbol{C}$ and the Green-strain tensor $\boldsymbol{E}$ are calculated:

$$\boldsymbol{F} = \begin{pmatrix} 1 & 0{\cdot}8 & 0 \\ 0 & 0{\cdot}6 & 0 \\ 0 & 0 & \beta \end{pmatrix}, \boldsymbol{C} = \begin{pmatrix} 1 & 0{\cdot}8 & 0 \\ 0{\cdot}8 & 1 & 0 \\ 0 & 0 & \beta^2 \end{pmatrix} \text{ and } \boldsymbol{E} = \frac{1}{2}(\boldsymbol{C} - \mathbf{1}) \tag{26}$$

The second Piola–Kirchhoff stress tensor becomes, according to the constitutive equation (16),

$$\tilde{\boldsymbol{T}} = \mu \begin{pmatrix} 1 & 0 & 0 \\ 0 & 1 & 0 \\ 0 & 0 & 1 \end{pmatrix} + \left[\frac{\lambda}{2} \ln(0{\cdot}36\beta^2) - \mu \right] \begin{pmatrix} \frac{25}{9} & -\frac{20}{9} & 0 \\ -\frac{20}{9} & \frac{25}{9} & 0 \\ 0 & 0 & \beta^{-2} \end{pmatrix} \tag{27}$$

The normal stress component in the z-direction shall be zero. This leads to

$$\frac{\lambda}{2} \ln(0{\cdot}36\beta^2) + \mu(\beta^2 - 1) = 0$$

This equation can be solved iteratively, for example by Newton's method, up to any accuracy for the unknown β^2. Once β^2 is known, the Green-strains are calculated from (26) and the second Piola–Kirchhoff stresses from (27). Numerical results are given in Table III.

REFERENCES

1. J. C. Simo and S. Rifai, 'A class of mixed assumed strain methods and the method of incompatible modes', *Int. j. numer. methods eng.*, **29**, 1595–1638 (1990).
2. N. Büchter, E. Ramm and D. Roehl, 'Three-dimensional extension of non-linear shell formulation based on the enhanced assumed strain concept', *Int. j. numer. methods eng.*, **37**, 2551–2568 (1994).
3. E. Ramm and A. Matzenmiller, 'Large deformation shell analyses based on the degeneration concept', in *State-of-the-art Texts on Finite Element Methods for Plate and Shell Structures*, T. J. R. Hughes and E. Hinton (Eds), Pineridge Press, Swansea, UK, 1986.
4. O. C. Zienkiewicz and R. L. Taylor, *The Finite Element Method*, 4th Edn, McGraw-Hill Book Company, London, 1989.
5. K. J. Bathe and E. Dvorkin, 'A four-node plate bending element based on Mindlin/Reissner plate theory and a mixed interpolation', *Int. j. numer. methods eng.*, **21**, 367–383 (1985).
6. N. Stander, A. Matzenmiller and E. Ramm, 'An assessment of assumed strain methods in finite rotation shell analysis', *Eng. Comput.*, **6**, 58–66 (1989).
7. J. C. Simo and K. S. Pister, 'Remarks on rate constitutive equations for finite deformation problems: Computational implications', *Comput. Methods Appl. Mech. Eng.*, **46**, 201–215 (1984).
8. J. Lubliner, 'A simple model of generalized plasticity', *Int. J. Solids Struct.*, **28**, 769–778 (1991).
9. C. Huettel and A. Matzenmiller, 'Numerical aspects of the plane stress case in generalized plasticity', *ZAMM*, submitted for publication, 1997.
10. G. Lührs, 'Randwertaufgaben der Viskoplastizität', PhD thesis, Department of Mechanical Engineering, University (Gh) of Kassel, *Report 1/1997*, 1997.

